

Organogermanium Reactive Intermediates. The Direct Detection and Characterization of Transient Germylenes and Digermenes in Solution

William J. Leigh,* Cameron R. Harrington, and Ignacio Vargas-Baca

Contribution from the Department of Chemistry, McMaster University,
1280 Main Street West, Hamilton, ON Canada L8S 4M1

Received June 22, 2004; E-mail: leigh@mcmaster.ca

Abstract: Diphenylgermylene (Ph_2Ge) and its Ge=Ge doubly bonded dimer, tetraphenyldigermene (**6a**), have been characterized directly in solution for the first time by laser flash photolysis methods. The germylene is formed via (formal) cheletropic photocycloreversion of 3,4-dimethyl-1,1-diphenylgermacyclopent-3-ene (**4a**), which is shown to proceed in high chemical (>95%) and quantum yield ($\Phi = 0.62$) by steady-state trapping experiments with methanol, acetic acid, isoprene, and triethylsilane. Flash photolysis of **4a** in dry deoxygenated hexane at 23 °C leads to the prompt formation of a transient assigned to Ph_2Ge ($\lambda_{\text{max}} = 500$ nm; $\epsilon_{\text{max}} = 1650 \text{ M}^{-1} \text{ cm}^{-1}$), which decays with second-order kinetics ($\tau \approx 3 \mu\text{s}$), with the concomitant growth of a second transient species that is assigned to digermene **6a** ($\tau \approx 40 \mu\text{s}$; $\lambda_{\text{max}} = 440$ nm). Analogous results are obtained from 1,1-dimesityl- and 1,1-dimethyl-3,4-dimethylgermacyclopent-3-ene (**4b** and **4c**, respectively), which afford Mes_2Ge ($\tau \approx 20 \mu\text{s}$; $\lambda_{\text{max}} = 560$ nm) and Me_2Ge ($\tau \approx 2 \mu\text{s}$; $\lambda_{\text{max}} = 480$ nm), respectively, as well as the corresponding digermenes, tetramesityl- (**6b**; $\lambda_{\text{max}} = 410$ nm) and tetramethyldigermene (**6c**; $\lambda_{\text{max}} = 370$ nm). The results for the mesityl compound are compared to the analogous ones from laser flash photolysis of the known Mes_2Ge /**6b** precursor, hexamesitylcyclotrigermane. The spectra of the three germylenes and two of the digermenes are in excellent agreement with calculated spectra, derived from time-dependent DFT calculations. Absolute rate constants for dimerization of Ph_2Ge and Mes_2Ge and for their reaction with *n*-butylamine and acetic acid in hexane at 23 °C are also reported.

Introduction

The chemistry of germylenes, the germanium analogues of carbenes, has been of considerable interest over the past thirty years. Several stable derivatives have been prepared and characterized, and their chemistry has been extensively studied.^{1–4} Numerous time-resolved spectroscopic studies of the reactivities of the simplest representatives in the gas phase or in solution have also been reported, including studies of the parent molecule (H_2Ge)^{5–15} and the dimethyl- (Me_2Ge)^{15–19} and diphenyl-

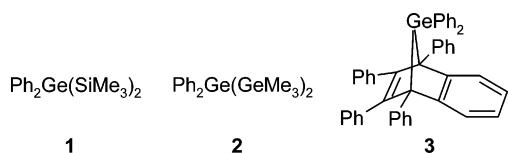
substituted (Ph_2Ge) derivatives,^{20–23} using photochemical methods to generate the germylene of interest and time-resolved UV–vis spectrophotometry to monitor it and determine rate constants for its reaction(s). Unfortunately, however, much of the reported work on Me_2Ge and Ph_2Ge in solution is characterized by a distinct lack of consistency in the spectroscopic properties and absolute reactivities of these transient species.²⁴ It has been suggested that this problem may originate in the photochemistry of the arylated oligogermane or disilylgermane precursors that have usually been used for their generation; compounds of this type are prone to competing photoreactions such as M–M' bond homolysis and [1,3]-sigmatropic rearrangements, which yield transient germanium-centered radicals and conjugated germene derivatives, respectively, in addition to the desired germylenes.^{24–27} These products are usually formed in minor yields, but they absorb strongly in the mid-

- (1) Neumann, W. P. *Chem. Rev.* **1991**, *91*, 311.
- (2) Barrau, J.; Rima, G. *Coord. Chem. Rev.* **1998**, *180*, 593.
- (3) Weidenbruch, M. *Eur. J. Inorg. Chem.* **1999**, *1999*, 373.
- (4) Tokitoh, N.; Okazaki, R. *Coord. Chem. Rev.* **2000**, *210*, 251.
- (5) Becerra, R.; Bogdanov, S. E.; Egorov, M. P.; Nefedov, O. M.; Walsh, R. *Chem. Phys. Lett.* **1996**, *260*, 433.
- (6) Becerra, R.; Bogdanov, S. E.; Egorov, M. P.; Faustov, V. I.; Nefedov, O. M.; Walsh, R. *J. Am. Chem. Soc.* **1998**, *120*, 12657.
- (7) Becerra, R.; Walsh, R. *Phys. Chem. Chem. Phys.* **1999**, *1*, 5301.
- (8) Alexander, U. N.; Trout, N. A.; King, K. D.; Lawrance, W. D. *Chem. Phys. Lett.* **1999**, *299*, 291.
- (9) Alexander, U. N.; King, K. D.; Lawrance, W. D. *Chem. Phys. Lett.* **2000**, *319*, 529.
- (10) Becerra, R.; Bogdanov, S. E.; Egorov, M. P.; Faustov, V. I.; Nefedov, O. M.; Walsh, R. *Can. J. Chem.* **2000**, *78*, 1428.
- (11) Becerra, R.; Bogdanov, S. E.; Egorov, M. P.; Faustov, V. I.; Nefedov, O. M.; Walsh, R. *Phys. Chem. Chem. Phys.* **2001**, *3*, 184.
- (12) Becerra, R.; Walsh, R. *J. Organomet. Chem.* **2001**, *636*, 49.
- (13) Becerra, R.; Bogdanov, S. E.; Egorov, M. P.; Faustov, V. I.; Promyslov, V. M.; Nefedov, O. M.; Walsh, R. *Phys. Chem. Chem. Phys.* **2002**, *4*, 5079.
- (14) Alexander, U. N.; King, K. D.; Lawrance, W. D. *Phys. Chem. Chem. Phys.* **2003**, *5*, 1557.
- (15) Becerra, R.; Egorov, M. P.; Krylova, I. V.; Nefedov, O. M.; Walsh, R. *Chem. Phys. Lett.* **2002**, *351*, 47.
- (16) Bobbitt, K. L.; Maloney, V. M.; Gaspar, P. P. *Organometallics* **1991**, *10*, 2772.

- (17) Mochida, K.; Kanno, N.; Kato, R.; Kotani, M.; Yamauchi, S.; Wakasa, M.; Hayashi, H. *J. Organomet. Chem.* **1991**, *415*, 191.
- (18) Mochida, K.; Tokura, S. *Bull. Chem. Soc. Jpn.* **1992**, *65*, 1642.
- (19) Becerra, R.; Bogdanov, S. E.; Egorov, M. P.; Lee, V. Y.; Nefedov, O. M.; Walsh, R. *Chem. Phys. Lett.* **1996**, *250*, 111.
- (20) Konieczny, S.; Jacobs, S. J.; Braddock Wilking, J. K.; Gaspar, P. P. *J. Organomet. Chem.* **1988**, *341*, C17.
- (21) Wakasa, M.; Yoneda, I.; Mochida, K. *J. Organomet. Chem.* **1989**, *366*, C1.
- (22) Mochida, K.; Yoneda, I.; Wakasa, M. *J. Organomet. Chem.* **1990**, *399*, 53.
- (23) Mochida, K.; Wakasa, M.; Hayash, H. *Phosphorus, Sulfur Silicon Relat. Elem.* **1999**, *150–151*, 237.
- (24) Bogdanov, S. E.; Egorov, M. P.; Faustov, V. I.; Nefedov, O. M. In *The chemistry of organic germanium, tin and lead compounds – Vol. 2*; Rappoport, Z., Ed.; John Wiley and Sons: New York, 2002; p 749.

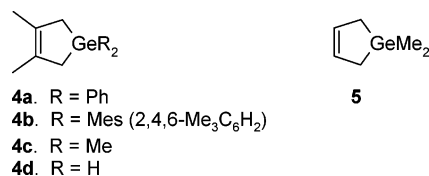
UV (400–500 nm), in exactly the same spectral region that the germynes of interest are expected to absorb. The proper interpretation of the results of these studies was also hindered by the nonavailability of quantitative kinetic data for the reactions of transient germynes, the first of these studies having been reported only relatively recently.²⁸ Complexation of the germylene with the precursor, solvent, or a photolysis co-product may also be a contributing factor.²⁴

For example, the UV spectrum of Ph_2Ge , generated by photolysis of **1–3** in a 3-methylpentane (3-MP) glass at 77 K, has been reported to exhibit $\lambda_{\text{max}} \approx 465$ nm.^{21,22,29,30} On the other hand, laser flash photolysis studies of **1** and **2** in cyclohexane solution at room temperature have afforded transient UV spectra that are different from those observed in 3-MP at 77 K and kinetic behavior that varies with the precursor.^{20–22} A species with $\lambda_{\text{max}} = 445$ nm and second-order lifetime (τ) of ca. 270 μs was assigned to Ph_2Ge in experiments using **1** as precursor,²⁰ while a transient with $\lambda_{\text{max}} = 450$ nm and (second-order) $\tau \approx 350$ ns was later assigned to the same species on the basis of similar experiments with **2**.^{21,22} Absolute rate constants for reaction of the species with hydridosilanes and 2,3-dimethyl-1,3-butadiene (DMB) differed by about an order of magnitude from the two precursors, and no evidence was found for reaction with ethanol. Steady-state photolysis experiments verified that Ph_2Ge extrusion is the major photoreaction of both **1** and **2** but also indicate that other competing processes occur as well. Unfortunately, to our knowledge benzogermanbornadiene **3**, the one precursor that is evidently not prone to the competing photoreactions that **1** and **2** undergo,^{30,31} has not yet been studied in fluid solution by time-resolved spectroscopic methods. The analogous literature on Me_2Ge is much more extensive than that on Ph_2Ge and is in a correspondingly greater state of confusion.²⁴

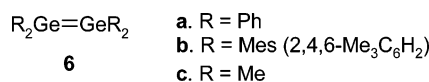


We have thus sought to develop an efficient photochemical precursor to Ph_2Ge that should not be prone to competing photoreactions of the types characteristic of arylated oligogermanes or disilylgermanes and is more straightforward to prepare and handle than molecules such as **3**. Herein we report the first results of our efforts, in the form of a steady-state and laser flash photolysis study of the photochemistry of 3,4-dimethyl-1,1-diphenylgermacyclopent-3-ene (**4a**) and the corresponding

1,1-dimesityl (**4b**; mesityl = 2,4,6-trimethylphenyl) analogue. These compounds were identified as potential precursors to diphenyl- and dimesitylgermylene, respectively, based simply on the fact that the 1,1-dihydro derivative (**4d**) and 1,1-dimethylgermacyclopent-3-ene (**5**) are known to extrude the corresponding germynes upon photolysis in the gas phase with 193 nm light, in amounts sufficient for their detection by time-resolved UV–vis spectroscopy.^{6,19,32} The dimesityl compound **4b** serves as a useful control against which to judge the results for **4a**, as the UV spectrum and reactivity of dimesitylgermylene (Mes_2Ge) have been previously characterized in solution²⁵ and in low-temperature matrixes,^{29,30,33} with quite good agreement between the various studies that have been reported. We have also carried out a preliminary study of the photochemistry of 1,1,3,4-tetramethylgermacyclopent-3-ene (**4c**) in solution by far-UV (193 nm) laser flash photolysis techniques,³⁴ to compare with previous gas- and solution-phase flash photolysis studies of Me_2Ge , and with the results obtained from 248 nm laser photolysis of the arylated derivatives **4a** and **4b**.



In this paper, we present the results of steady-state (lamp) photolysis of these compounds in the presence of various germylene trapping reagents, which show that this class of precursor does indeed constitute a highly efficient, essentially quantitative source of the corresponding germylene derivative. The germynes and their corresponding digermene dimers (**6a–c**) have been detected and characterized by laser flash photolysis methods, using time-dependent DFT calculations to support the transient assignments. The assignment of tetraphenyldigermene



(**6a**) is further supported by product studies using high-intensity laser excitation, which enables competitive trapping of the digermene and the germylene from which it is formed. Absolute rate constants for dimerization of the two diarylgermylenes and for reaction with *n*-butylamine and acetic acid are also reported, the latter to provide further support for the transient assignments. The results reported here form the basis of a more detailed kinetic study of the reactions of Ph_2Ge and **6a** with a broad range of reactants, including amines, alcohols, carboxylic acids, ketones, alkenes, alkynes, dienes, Group 14 hydrides, halocarbons, and oxygen, which will be reported separately.³⁵

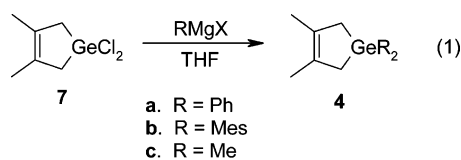
Results and Discussion

Compounds **4a–c** were prepared in 80–90% yield by reaction of the corresponding aryl or alkyl Grignard reagent with 1,1-dichloro-3,4-dimethylgermacyclopent-3-ene (**7**; eq 1), which was prepared in high yield via a two-step procedure

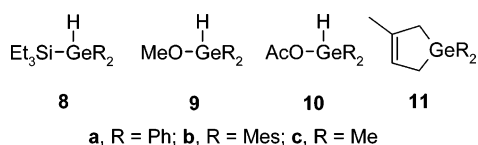
- (25) Toldt, N. P.; Leigh, W. J.; Kollegger, G. M.; Stibbs, W. G.; Baines, K. M. *Organometallics* **1996**, *15*, 3732.
 (26) Baines, K. M.; Cooke, J. A.; Dixon, C. E.; Liu, H.; Netherton, M. R. *Organometallics* **1994**, *13*, 631.
 (27) Leigh, W. J.; Toldt, N. P.; Apodeca, P.; Castruita, M.; Pannell, K. H. *Organometallics* **2000**, *19*, 3232.
 (28) Toldt, N. P.; Leigh, W. J. *J. Am. Chem. Soc.* **1998**, *120*, 1172.
 (29) Ando, W.; Tsumuraya, T.; Sekiguchi, A. *Chem. Lett.* **1987**, 317.
 (30) Ando, W.; Itoh, H.; Tsumuraya, T. *Organometallics* **1989**, *8*, 2759.
 (31) Kocher, J.; Lehnig, M.; Neumann, W. P. *Organometallics* **1988**, *7*, 1201.
 (32) Note added in proof: We recently learned that preliminary details of the photolysis of **4a** in the presence of isoprene were reported several years ago in a conference proceeding. See: Bobbitt, K. L.; Lei, D.; Maloney, V. M.; Parker, B. S.; Raible, J. M.; Gaspar, P. P. In *Frontiers of organogermanium, -tin and -lead chemistry*; Lukevics, E.; Ignatovich, L., Eds.; Latvian Institute of Organic Synthesis: Riga, 1993; p 41. We thank Professor P. P. Gaspar for bringing this to our attention and for providing a reprint of the article.

- (33) Ando, W.; Itoh, H.; Tsumuraya, T.; Yoshida, H. *Organometallics* **1988**, *7*, 1880.
 (34) Kerst, C.; Byloos, M.; Leigh, W. J. *Can. J. Chem.* **1997**, *75*, 975.
 (35) Leigh, W. J.; Harrington, C. R. Di- and Trivalent Organogermanium Reactive Intermediates. Kinetics and Mechanisms of Some Reactions of Diphenylgermylene and Tetraphenyldigermene in Solution. To be published.

starting from germanium tetrachloride. The three compounds exhibited spectroscopic and analytical properties similar to previously reported data.^{36–38}

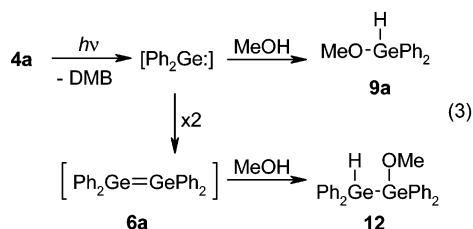
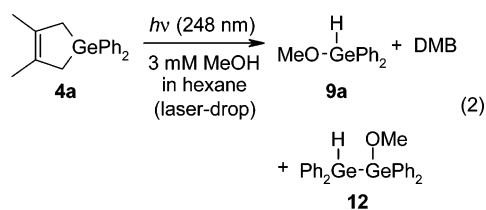


Photolysis of argon-saturated cyclohexane-*d*₁₂ solutions of **4a** (0.05 M) in the presence of 0.5 M triethylsilane, methanol, acetic acid, or isoprene, with low-pressure mercury lamps (254 nm), led to the formation of 2,3-dimethyl-1,3-butadiene (DMB) and equal yields of the expected germylene-trapping products **8a**, **9a**, **10a**, and **11a**, respectively. The products, which were in



each case formed in chemical yields exceeding 95% at conversions below ca. 20%, were identified by ¹H NMR and FTIR spectroscopy and GC/MS analyses of the crude reaction mixtures. The assignments were corroborated by comparisons to authentic samples in three of the four cases (**8a**, **9a**, **11a**); the acetoxygermane (**10a**) could not be successfully isolated. Similarly, compounds **9b** and **11b** were obtained along with DMB in quantitative yields upon photolysis of cyclohexane-*d*₁₂ solutions of **4b** in the presence of methanol or isoprene, under similar conditions to those used for the photolyses of **4a**. Finally, 214 nm photolysis of deoxygenated solutions of **4c** (0.02 M) in cyclohexane-*d*₁₂ containing methanol (0.035 M) or isoprene (0.005 M) afforded DMB and roughly equal amounts of **9c** or **11c**, respectively, according to ¹H NMR, GC, and/or GC/MS analysis of the crude product mixtures between ca. 3 and 10% conversion of the starting material.

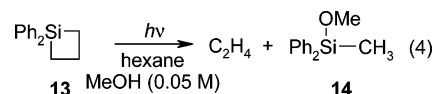
Preparative laser photolysis of a deoxygenated solution of **4a** (0.003 M) in hexane containing MeOH (0.003 M), with the focused pulses from a KrF excimer laser (248 nm; ca. 25 ns, ca. 150 mJ) in a laser-drop apparatus,³⁹ afforded a mixture of DMB, **9a**, and 1-methoxy-1,1,2,2-tetraphenyldigermene (**12**; eq 2). The conversion of **4a** in this experiment was ca. 2%. The



products were identified by (600 MHz) ¹H NMR spectroscopy

(see Supporting Information), with the identity of **12** being confirmed by spiking the photolyzed mixture with a small amount of an authentic, independently prepared sample of the compound. The relative yields of **12** and **9a** in these experiments varied depending on the laser intensity and alcohol concentration, with the yield of **12** relative to that of **9a** being significantly lower (or not detectable at all) in experiments carried out at lower laser intensities or in the presence of higher concentrations of MeOH. For example, only **9a** could be detected upon photolysis of **4a** in the presence of 0.03 M MeOH, under otherwise identical conditions as required to produce **12** and **9a** in a ratio of ca. 1:4 from photolysis of **4a** in the presence of 0.003 M MeOH. These results are consistent with competitive trapping of Ph₂Ge with MeOH and dimerization to form tetraphenyldigermene (**6a**), which is subsequently trapped as the expected methanol addition product (**12**; eq 3). The success of the experiment depends on the use of a sufficiently high laser flux to ensure that Ph₂Ge is formed in relatively high concentrations and sufficiently low methanol concentrations to ensure that dimerization of the germylene competes effectively with trapping by the alcohol.

The quantum yield for formation of **9a** from **4a** was determined to be Φ_{Ph₂Ge} = 0.62 ± 0.08, by merry-go-round photolysis of deoxygenated, optically matched solutions of **4a** (0.037 M) and 1,1-diphenylsilacyclobutane (**13**; 0.043 M) in methanolic (0.5 M) cyclohexane-*d*₁₂ solution, with periodic monitoring of the photolyzates by ¹H NMR spectroscopy between 0 and ca. 25% conversion of **4a**. The photolysis of **13** under these conditions yields ethylene and methoxymethyl-diphenylsilane (**14**; eq 4) with a quantum yield of Φ₁₄ = 0.21 ± 0.02.⁴⁰



Laser Flash Photolysis of 4a–c. The Direct Detection of Germylenes and Digermenes. Laser flash photolysis of continuously flowing, deoxygenated solutions of **4a** (ca. 0.003 M) in dried hexane with the pulses from a KrF excimer laser (248 nm, ca. 25 ns, ca. 100 mJ) leads to the formation of two transient species. This is illustrated in Figure 1a, in the form of transient absorption spectra recorded in point-by-point fashion 55–170 ns and 3.0–3.2 μs after the laser pulse. The first transient is formed with the pulse and exhibits an absorption maximum at λ_{max} = 500 nm. The signal due to this species is superimposed on that of a second, much longer-lived transient, which exhibits λ_{max} = 440 nm, grows in with approximate second-order kinetics over ca. 2 μs, and then decays with mixed first- and second-order kinetics and a lifetime τ ≈ 40 μs. The absorptions due to this second transient overlap considerably with those of the initially formed transient, so much so that the kinetic form of the decay of the initially formed species cannot be determined from the raw data recorded at 500 nm. However, the decay profile of the initially formed transient could be

(36) Mazerolles, P.; Manuel, G. *Bull. Soc. Chim. Fr.* **1965**, *56*, 327.

(37) Tsumuraya, T.; Kabe, Y.; Ando, W. *J. Organomet. Chem.* **1994**, *482*, 131.

(38) Schriewer, M.; Neumann, W. P. *J. Am. Chem. Soc.* **1983**, *105*, 887.

(39) Banks, J. T.; Garcia, H.; Miranda, M. A.; Perez-Prieto, J.; Scaiano, J. C. *J. Am. Chem. Soc.* **1995**, *117*, 5049.

(40) Toltl, N. P.; Stradiotto, M. J.; Morkin, T. L.; Leigh, W. J. *Organometallics* **1999**, *18*, 5643.

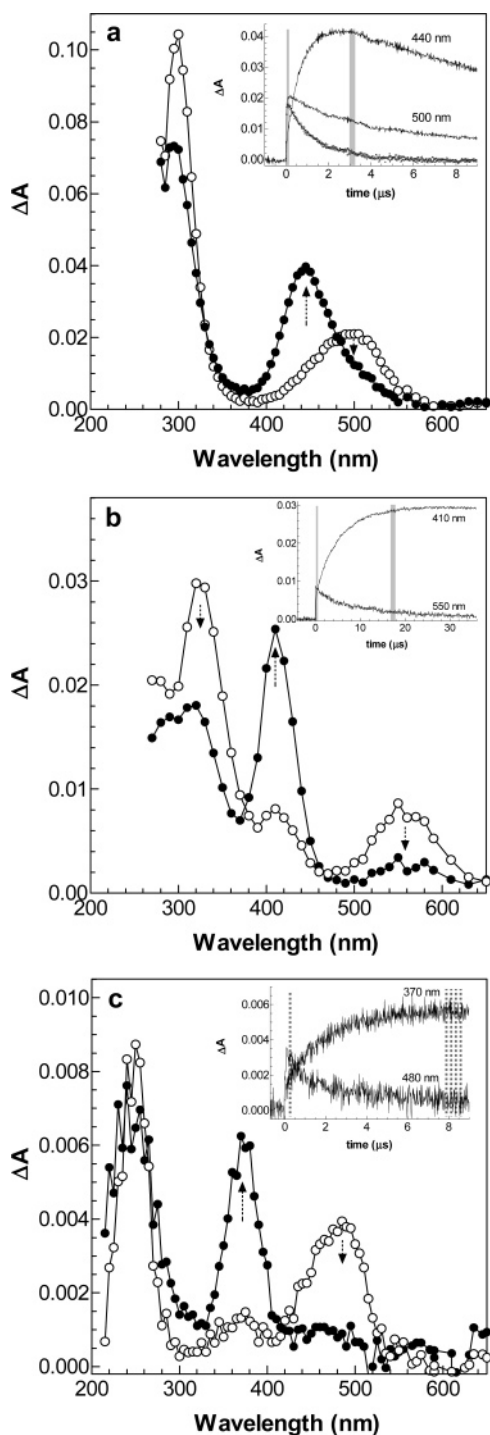


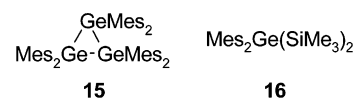
Figure 1. Transient UV absorption spectra from laser flash photolysis of (a) a 0.003 M solution of **4a** in dried, deoxygenated hexane solution at 23 °C, recorded 55–170 ns (○) and 3.0–3.2 μs (●) after the (248 nm) laser pulse; (b) a 0.004 M solution of **4b** under similar conditions, recorded 50–400 ns (○) and 16.8–17.8 μs (●) after the (248 nm) laser pulse; and (c) a 5×10^{-5} M solution of **4c** in dried, deoxygenated hexane solution at 23 °C, recorded 50–400 ns (○) and 7.8–8.6 μs (●) after the (193 nm) laser pulse. The inserts show typical transient absorption profiles recorded at (a) 500 and 440 nm; (b) 550 and 410 nm; and (c) 480 and 370 nm. The third transient decay profile shown in the insert in part a was calculated by subtracting the 440 nm growth/decay profile ($\times 0.25$) from the 500 nm decay profile.

extracted from the raw decays recorded at 500 nm by subtraction of the profile recorded at 440 nm, scaled by the approximate relative absorbances of the 440 nm species at 500 and 440 nm (see Figure 1a, insert; $\epsilon_{500}/\epsilon_{440} \approx 0.25$). The procedure is a crude

one, partly because the 440 nm transient absorption contains minor contributions from the 500 nm species; accordingly, it afforded a decay profile that fit acceptably to mixed first- and second-order kinetics with a lifetime $\tau \approx 1.5 \mu\text{s}$. Traces recorded at 530 nm were ca. 40% weaker than those recorded at 500 nm, but fit reasonably well to second-order kinetics under scrupulously dry, deoxygenated conditions with a (second-order) lifetime of ca. $3 \mu\text{s}$ (vide infra). The reasonably good qualitative agreement between the decay rate of the 500 nm species and the apparent growth rate of the 440 nm species is consistent with the latter being formed from the former via a second-order kinetic process, allowing assignment of the initially formed transient to diphenylgermylene (Ph_2Ge) and the subsequently formed one to its dimer, tetraphenyldigermene (**6a**). We note that quantitative agreement between the germylene decay and digermene growth kinetics can only be expected under circumstances where the digermene is stable over a much longer time scale than that in which it is formed (and it is not; see Figure 1a, insert) and where other reactive pathways (e.g., reaction with impurities, the precursor, the photolysis coproduct, or the dimerization product as it is formed) do *not* compete with dimerization. This will be discussed in more detail later in the paper.

The transient spectra shown in Figure 1a both contain a second, significantly more intense absorption band centered at $\lambda_{\text{max}} = 290\text{--}300$ nm, a result of the fact that transient decay profiles recorded at this wavelength consist of both a fast and slow decay component, superimposed on a stable residual absorption that is most likely associated with oligomerization products of **6a**. The decay characteristics of the signals in this region of the spectrum are too complex for reliable assignments to be made at this time.

Similarly, flash photolysis of a flowed, deoxygenated 0.004 M solution of **4b** in dry hexane affords the known dimesitylgermylene ($\lambda_{\text{max}} = 325, 560$ nm),^{25,30} which decays over a similar time scale as the growth of absorptions due to tetramesityldigermene (**6b**; $\lambda_{\text{max}} = 410$ nm),^{25,30,41} as illustrated in Figure 1b. Again, only qualitative agreement is observed between the decay kinetics of the germylene absorption and the apparent growth kinetics of the digermene, but both fit reasonably well to second-order kinetics and exhibit decay and growth constants that match each other within a factor of 2. The optical yield of dimesitylgermylene from **4b** is significantly higher than that obtained from either hexamesitylcyclotrigermane (**15**) or bis-(trimethylsilyl)dimesitylgermane (**16**), which have both been studied previously by our group by flash photolysis methods.²⁵ However, the yield of **6b** by dimerization of Mes_2Ge : is significantly lower than that obtained from **15** under similar conditions, and the digermene appears to be unstable, decaying with a pseudo-first-order lifetime of ca. 2 ms (vide infra).



Finally, far-UV (193 nm) laser flash photolysis of deoxygenated hexane solutions of **4c** (ca. 5×10^{-5} M) afforded similar transient behavior to that described above for **4a** and **4b**. The signals obtained in these experiments were substantially weaker,

(41) Masamune, S.; Hanzawa, Y.; Williams, D. J. *J. Am. Chem. Soc.* **1982**, *104*, 6136.

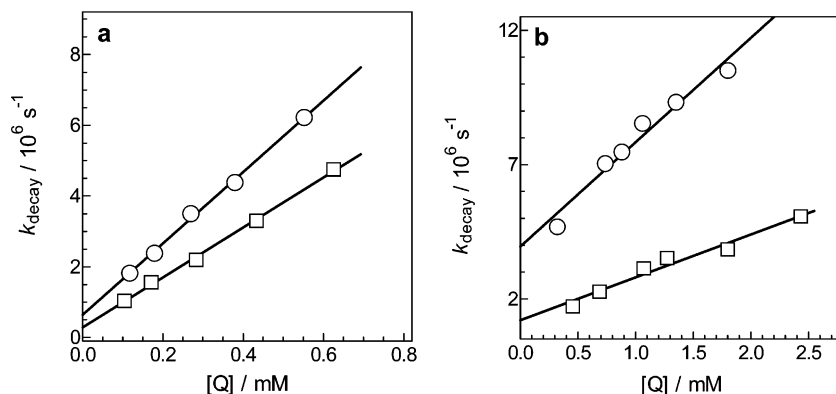
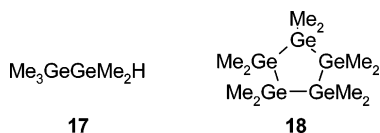


Figure 2. Pseudo-first-order rate constants for the decay of Ph_2Ge (O) and Mes_2Ge (□) in the presence of (a) $n\text{-BuNH}_2$ and (b) AcOH in dried hexane solution at 23 °C, at concentrations at which the formation of **6a** and **6b** is more than 80% quenched.

however, due most likely to a combination of lower quantum yield, weaker excitation pulse energy (roughly half that at 248 nm), and screening of the excitation light by the solvent (which accounts for ca. 30% of the solution absorbance at 193 nm). Transient spectra and typical decay/growth profiles are shown in Figure 1c; they consist of a prompt, relatively weak absorption centered at 480 nm, which decays with approximate second-order kinetics ($\tau \approx 2 \mu\text{s}$) to form a second species that absorbs at $\lambda_{\text{max}} = 370 \text{ nm}$ and then decays over the next several hundred microseconds. The absorption spectrum of the initially formed transient is similar to that reported previously for Me_2Ge in the gas-phase (from laser photolysis of **5b** and pentamethyldigermene (**17**))^{15,19} and in solution (from laser photolysis of decamethylcyclopentagermane (**18**)).¹⁸ That of the second transient matches the spectrum previously assigned to tetramethyldigermene (**6c**) by Mochida and co-workers.^{17,42}



The intensities of the signals observed in experiments with **4a** and **4b** depend critically on the concentration of water in the solvent, with the strongest signals being observed with samples of hexane that had been dried by distillation from lithium aluminum hydride or sodium/potassium amalgam, using oven-baked glassware and sample cells. These effects are much more pronounced for **4a** than for **4b** and are indicative of reaction of the germylenes with water or other hydroxylic impurities, which results in reductions in the intensities of the signals observed for both the germylene and the digermene. For example, laser flash photolysis of **4a** in a sample of untreated, HPLC-grade hexane ($[\text{H}_2\text{O}] \approx 1.5 \text{ mM}$) afforded signals due to Ph_2Ge and **6a** that were roughly 55% and 75% weaker, respectively, than those recorded in the dried solvent. Interestingly, the bulk decay and growth kinetics of the two species are approximately the same under the two sets of conditions, suggestive of a rapid equilibrium between the free germylene and its complex with water.³⁵ Indeed, such a phenomenon was suggested several years ago by Neumann and co-workers for Me_2Ge ,⁴³ and spectroscopic evidence for the formation of Lewis

Table 1. Absolute Rate Constants for Reaction of Diarylgermylenes (Ph_2Ge and Mes_2Ge) and Tetraaryldigermenes (**6a** and **6b**) with $n\text{-BuNH}_2$ and AcOH in Dried Hexane Solution at 23 °C

Q	$k_Q/10^9 \text{ M}^{-1} \text{ s}^{-1}$		$k_0/10^9 \text{ M}^{-1} \text{ s}^{-1}$	
	Ph_2Ge^a	Mes_2Ge^a	6a ^a	6b ^b
$n\text{-BuNH}_2$	10.1 ± 0.6	7.0 ± 0.30	2.4 ± 0.3	$< 7 \times 10^{-7}$
AcOH	3.9 ± 0.7	1.6 ± 0.3	< 0.04	$< 10^{-7}$

^a Using **4a** or **4b** as precursor. ^b Using **15** as precursor.

acid–base complexes between diarylgermylenes and aliphatic alcohols in low-temperature matrixes has been reported by Ando and co-workers.³⁰ On the other hand, the presence of residual oxygen resulting from incomplete deoxygenation had only small effects on the intensities and decay profiles of the signals due to Ar_2Ge and the corresponding digermenes.

Addition of n -butylamine ($n\text{-BuNH}_2$) or acetic acid (AcOH) to the solutions of **4a** and **4b** caused enhancements in the decay rates of the signals assigned to Ph_2Ge and Mes_2Ge and reductions in the maximum intensities of the signals due to **6a** and **6b**, in proportion to the concentration of added reagent. This is consistent with trapping of the germylenes by $n\text{-BuNH}_2$ and AcOH , in competition with dimerization to the corresponding digermenes. At concentrations above those required to reduce the digermene signal intensities to less than ca. 20% of their values in the absence of added reagent (ca. 0.1–0.5 mM), the decay profiles of the germylene signals followed clean first-order kinetics and plots of the pseudo-first-order decay rate constants (k_{decay}) vs concentration were linear. Typical plots are shown in Figure 2. The linear behavior is consistent with the relationship of eq 5, where k_Q is the second-order rate constant for reaction of the germylene with the added reagent (Q) and k_0 is the (hypothetical) pseudo-first-order rate constant for germylene decay in the absence of Q. The absolute rate constants for reaction of Ph_2Ge and Mes_2Ge with these two reagents are collected in Table 1.

$$k_{\text{decay}} = k_0 + k_Q[\text{Q}] \quad (5)$$

In the case of the amine, acceleration of the decay of the signal due to **6a** and a change to first-order decay kinetics was evident over the (low) concentration ranges where the species could still be detected. A plot of k_{decay} vs $[n\text{-BuNH}_2]$ was linear (see Figure 3) and afforded a quenching rate constant of $k_Q = (2.4 \pm 0.3) \times 10^9 \text{ M}^{-1} \text{ s}^{-1}$. No such acceleration was evident in the decay of **6b** over a similar concentration range in amine.

(42) Mochida, K.; Kayamori, T.; Wakasa, M.; Hayashi, H.; Egorov, M. P. *Organometallics* **2000**, *19*, 3379.

(43) Klein, B.; Neumann, W. P.; Weisbeck, M. P.; Wienken, S. *J. Organomet. Chem.* **1993**, *446*, 149.

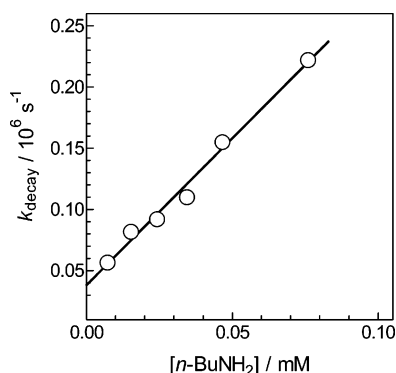
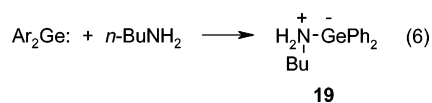


Figure 3. Pseudo-first-order rate constants for the decay of digermene **6a** in the presence of *n*-BuNH₂ in dried hexane solution at 23 °C, over the concentration range at which its formation is less than 90% quenched. The solid line represents the best (linear least squares) fit of the data to eq 5.

A slight acceleration of the decay rates of **6a** was evident in the experiments with AcOH, allowing assignment of an upper limit of $\sim 4 \times 10^7 \text{ M}^{-1} \text{ s}^{-1}$ for the rate constant for its reaction with AcOH. Upper limits for the rate constants for reaction of these two reagents with **6b** are on the order of $10^2 \text{ M}^{-1} \text{ s}^{-1}$ and were established using **15** as the precursor.

These data are a subset of an extensive study of the kinetics and mechanisms of the reactions of these species with a variety of germylene and digermene scavengers, which has been carried out in parallel with the present work and will be reported separately.³⁵ They are included here because they effectively rule out a number of possible alternative transient assignments, such as excited triplet states, free radicals, or radical ions. On the other hand, both amines and carboxylic acids are known to react with transient germylenes.⁴³ Absolute rate constants have not yet been reported in any case, however.^{30,33}

In both cases, addition of *n*-BuNH₂ also resulted in the formation of a new transient species that decayed with mixed-order kinetics and exhibited $\lambda_{\text{max}} \leq 325 \text{ nm}$. We tentatively assign these species to the Lewis acid–base complexes between Ar₂Ge and the amine (**19**; eq 6), as complexes of this type have been reported previously upon generation of these and other germylenes in low-temperature glasses.^{30,33} Interestingly, steady-



state photolysis of cyclohexane-*d*₁₂ solutions of **4a** containing *n*-BuNH₂ leads to the formation of oligomeric material and very small amounts of nitrogen-containing products that are detectable only at higher conversions of the starting material. On the other hand, the reaction with AcOH is quite clean, resulting in the exclusive formation of the O–H insertion product (e.g., **10a** from Ph₂Ge) with no detectable intermediates. It should be noted that the carboxylic acid exists as a mixture of the monomeric species and the hydrogen-bonded dimer in hexane even at sub-millimolar bulk concentrations.⁴⁴ Replotting the decay rate constants of Figure 2b against either the monomeric AcOH concentration or the sum of the monomer and dimer concentrations (calculated using the monomer–dimer equilibrium constant of Fujii and co-workers for acetic acid in hexane at 25 °C, $K = 3200 \text{ M}^{-1}$ ⁴⁴) led to significant improvements in the quality of

the fits and absolute rate constants that are ca. 4 and 2 times greater, respectively, than the value measured using the bulk concentrations. However, we have no information on which to base an opinion on the relative reactivities of the monomeric and dimeric forms of AcOH toward O–H insertion by the germylene.

The course of the reaction of *n*-BuNH₂ with **6a** has not yet been ascertained but can most likely be identified as 1,2-addition across the Ge=Ge bond. The substantially greater reactivity of **6a** toward the amine compared to the carboxylic acid is suggestive of a mechanism involving initial nucleophilic attack at germanium, analogous to the addition of nucleophiles to disilenes.^{45,46} As expected, **6b** is several orders of magnitude less reactive than **6a**, probably owing mainly to the greater degree of steric protection of the Ge=Ge bond that is afforded by the mesityl substituents in the molecule.

The extinction coefficient for Ph₂Ge in hexane solution at the absorption maximum was determined by benzophenone actinometry.^{47,48} The method involves comparing the initial ΔA value at 500 nm ($\Delta A_{500,0}$) due to Ph₂Ge to that recorded at 525 nm for a solution of benzophenone, whose irradiation yields the triplet state ($\lambda_{\text{max}} = 525 \text{ nm}$, $\epsilon_{525\text{nm}} = 6250 \pm 1250 \text{ M}^{-1} \text{ cm}^{-1}$) with unit quantum yield.⁴⁹ The substrate and actinometer solutions were optically matched at the laser wavelength (248 nm) to ensure equal light absorption, both solutions were flowed, and the laser intensity was varied using neutral density filters. As expected, plots of $\Delta A_{\lambda,0}$ vs laser intensity at the two monitoring wavelengths were linear for both compounds at low to moderate laser intensities (see Supporting Information).⁴⁸ The extinction coefficient for Ph₂Ge at its absorption maximum was then calculated from the relative slopes of the plots and the quantum yield for formation of Ph₂Ge determined above. Duplicate determinations yielded an average value of $\epsilon_{\text{Ph}_2\text{Ge},500} = 1650 \pm 390 \text{ M}^{-1} \text{ cm}^{-1}$.

The maximum absorption intensities at 440 nm were also measured during these experiments; plots of $\Delta A_{440,\text{max}}$ vs laser intensity also showed good linearity, and the average slopes afforded an estimate of $\epsilon_{\text{6a},440} = 5970 \pm 1250 \text{ M}^{-1} \text{ cm}^{-1}$ for **6a**. However, this value was calculated without consideration for the fact that **6a** decays over the time scale in which it is formed and with the assumption that it is formed from Ph₂Ge in quantitative yield, which we do not believe to be true (vide infra). It should thus be considered a lower limit, differing from the true value by at least a factor of 2.

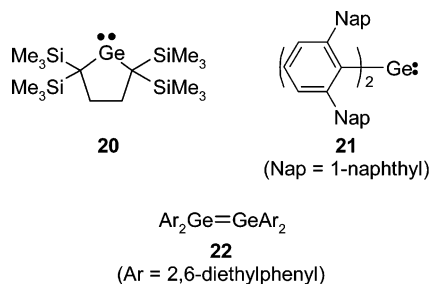
As mentioned above, Ph₂Ge has previously been reported to exhibit a UV absorption maximum at 445–450 nm in hydrocarbon solvents at room temperature^{20–22,50} and at 465 nm in hydrocarbon glasses at 77K,^{22,30} in contrast to the results reported above from laser photolysis of **4a**. Previous assignments of the UV spectrum of **6a** are similarly contradictory, with

- (45) Sakurai, H. In *The Chemistry of Organic Silicon Compounds*; Rappoport, Z., Apeloig, Y., Eds.; Wiley and Sons: Ltd: 1998; pp 827–855.
- (46) Morkin, T. L.; Owens, T. R.; Leigh, W. J. In *The chemistry of organic silicon compounds, Volume 3*; Rappoport, Z., Apeloig, Y., Eds.; John Wiley and Sons: New York, 2001; pp 949–1026.
- (47) Carmichael, I.; Hug, G. L. In *CRC handbook of organic photochemistry, Vol. 1*; Scaiano, J. C., Ed.; CRC Press: Boca Raton, FL, 1989; pp 369–404.
- (48) Wintgens, V.; Johnston, L. J.; Scaiano, J. C. *J. Am. Chem. Soc.* **1988**, *110*, 5117.
- (49) Carmichael, I.; Helman, W. P.; Hug, G. L. *J. Phys. Chem. Ref. Data* **1987**, *16*, 239.
- (50) Mochida, K.; Wakasa, M.; Nakadaira, Y.; Sakaguchi, Y.; Hayashi, H. *Organometallics* **1988**, *7*, 1869.

(44) Fujii, Y.; Yamada, H.; Mizuta, M. *J. Phys. Chem.* **1988**, *92*, 6768.

values of λ_{\max} varying between 320 nm²⁰ and 450 nm²³ in hydrocarbon solution at room temperature. Similarly, there is poor consensus as to the position of the UV spectral maximum of Me₂Ge, with reported values varying between 320 and 490 nm.²⁴ The spectra reported here for the three germylenes are similar to those reported previously for the corresponding silylene derivatives Me₂Si (λ_{\max} = 465 nm in cyclohexane at ~20 °C^{51,52}), Ph₂Si (λ_{\max} = 495 nm in 3-methylpentane at 77 K⁵³), and Mes₂Si (λ_{\max} = 580 nm in cyclohexane at 25 °C⁵⁴); analogous similarities exist between the spectra of **6b** and **6c** and those of tetramesityldisilene (λ_{\max} = 420 nm in cyclohexane at 25 °C^{54a}) and tetramethyldisilene (λ_{\max} = 360 nm in cyclohexane at 22 °C^{54b}), respectively. A reinvestigation of the time-resolved spectroscopy of **1** and a similar study of an analogue of **3** is in progress; the preliminary results of this work are in fact fully compatible with the present results for **4a**.⁵⁵ Nevertheless, we decided to compare the germylene and digermene spectra obtained in the present work with the results of time-dependent density functional theory (TD-DFT) calculations, to establish the validity of our transient assignments further.

TD-DFT Calculations of the Electronic Spectra of Germylenes and Digermenes. The choice of basis set and density functional used in the calculations was made by first carrying out a series of geometry optimizations for the stable germylene **20** and comparing the results to the reported single-crystal X-ray structure of the compound.⁵⁶ Four functionals were investigated,



using uncontracted Slater-type orbitals (STOs) of triple- ζ quality as basis functions (see Supporting Information). The exchange and correlation functionals of Perdew and Wang (PW91) were found to afford the best agreement with the reported crystallographic data for **20** and were thus used in subsequent geometry optimizations for the other species investigated. The calculated R–Ge distances and R–Ge–R bond angles (R = H or C) for H₂Ge, Me₂Ge, and Ph₂Ge (see Supporting Information) and vibrational frequencies for H₂Ge agreed well with the results of previous calculations at other levels of theory^{1,57–61} and with experimental structural data for H₂Ge⁶² and the stable diarylgermylene bis[2,6-bis(1-naphthyl)phenyl]germylene (**21**).⁵⁹ Simi-

larly, the calculated structural parameters for digermene (Ge₂H₄) and **6c** agree well with the results of previous calculations for the two molecules.^{63–68} In the cases of **6a** and **6b**, the calculated bond distances are generally in good agreement with crystallographic data reported for tetrakis(2,6-diethylphenyl)digermene (**22**),⁶⁹ but the Ge=Ge distances are overestimated by as much as 0.1 Å. More serious deviations from the crystallographic structure are observed in the bond and torsional angles about the germanium atoms, and the calculations predict a much greater degree of pyramidalization at germanium than is observed in the crystal structure of **22**.

Although the dimensions of the structures calculated here for **6a** and **6b** fall within the experimentally observed range for **22** and are in agreement with theoretical studies of smaller molecules,^{70–72} the results for all digermenes must be taken with caution. The accurate prediction of the structure of compounds containing double bonds between heavy Group 14 elements is notoriously difficult; the potential surfaces are fairly flat⁷³ resulting in great variability of the Ge=Ge bond distance (2.213–2.454 Å), the pyramidalization angle (~0–45°), and the twist angle (<10°).^{3,69,74,75}

Preliminary TD-DFT calculations were then carried out for **20** to identify the best basis set and exchange-correlation model for the prediction of electronic transitions in these species. The best balance between accuracy (as defined by the degree of agreement with the experimental UV spectrum⁵⁶) and computation time was obtained using the statistical average of different model potentials for occupied KS orbitals (SAOP)^{76,77} with triple- ζ double-polarization basis sets and the inclusion of relativistic effects (ZORA formalism). The basis sets were reduced to triple- ζ single-polarization to expedite the calculations for the digermenes.

The calculated lowest energy transitions in the UV–visible spectra of the three germylenes and the corresponding digermenes studied in this work are collected in Table 2, along with the experimental absorption maxima determined by laser flash photolysis of **4a–c**. Calculated and experimental λ_{\max} values for **20** are also included in the table. There is excellent

- (51) Levin, G.; Das, P. K.; Lee, C. L. *Organometallics* **1988**, *7*, 1231.
 (52) Levin, G.; Das, P. K.; Bilgrien, C.; Lee, C. L. *Organometallics* **1989**, *8*, 1206.
 (53) Michalczyk, M. J.; Fink, M. J.; De Young, D. J.; Carlson, C. W.; Welsh, K. M.; West, R.; Michl, J. *Silicon, Germanium, Tin and Lead Compounds* **1986**, *9*, 750.
 (54) (a) Conlin, R. T.; Netto-Ferreira, J. C.; Zhang, S.; Scaiano, J. C. *Organometallics* **1990**, *9*, 1332. (b) Yamaji, M.; Hamanishi, K.; Takahashi, T.; Shizuka, H. *J. Photochem. Photobiol., A* **1994**, *81*, 1.
 (55) Leigh, W. J.; Chan, B. R.; Harrington, C. R.; Gaspar, P. P. Time-resolved spectroscopic studies of the photochemistry of some diphenylgermylene precursors. To be submitted.
 (56) Kira, M.; Ishida, S.; Iwamoto, T.; Ichinohe, M.; Kabuto, C.; Ignatovich, L.; Sakurai, H. *Chem. Lett.* **1999**, 263.

- (57) BelBruno, J. J. *Heteroatom. Chem.* **1998**, *9*, 195.
 (58) Su, M.-D.; Chu, S.-Y. *J. Am. Chem. Soc.* **1999**, *121*, 11478.
 (59) Wegner, G. L.; Berger, R. J. F.; Schier, A.; Schmidbaur, H. *Organometallics* **2001**, *20*, 418.
 (60) Szabados, A.; Hargittai, M. *J. Phys. Chem. A* **2003**, *107*, 4314.
 (61) Lemierre, V.; Chrostowska, A.; Dargelos, A.; Baylere, P.; Leigh, W. J.; Harrington, C. R. *Appl. Organomet. Chem.* **2004**, *18*, 000.
 (62) Karolczak, J.; Harper, W. W.; Grev, R. S.; Clouthier, D. J. *J. Chem. Phys.* **1995**, *103*, 2839.
 (63) Liang, C.; Allen, L. C. *J. Am. Chem. Soc.* **1990**, *112*, 1039.
 (64) Grev, R. S.; Schaefer, H. F., III *Organometallics* **1992**, *11*, 3489.
 (65) Chen, W.-C.; Su, M.-D.; Chu, S.-Y. *Organometallics* **2001**, *20*, 564.
 (66) Malcolm, N. O. J.; Gillespie, R. J.; Popelier, P. L. A. *J. Chem. Soc., Dalton Trans.* **2002**, 3333.
 (67) Mosey, N. J.; Baines, K. M.; Woo, T. K. *J. Am. Chem. Soc.* **2002**, *124*, 13306.
 (68) Wang, X.; Andrews, L.; Kushto, G. P. *J. Phys. Chem. A* **2002**, *106*, 5809.
 (69) Snow, J. T.; Murakami, S.; Masamune, S.; Williams, D. J. *Tetrahedron Lett.* **1984**, *25*, 4191.
 (70) Trinquier, G. *J. Am. Chem. Soc.* **1990**, *112*, 2130.
 (71) Grev, R. S.; Schaefer, H. F., III; Baines, K. M. *J. Am. Chem. Soc.* **1990**, *112*, 9458.
 (72) Windus, T. L.; Gordon, M. S. *J. Am. Chem. Soc.* **1992**, *114*, 9559.
 (73) Jacobsen, H.; Ziegler, T. *J. Am. Chem. Soc.* **1994**, *116*, 3667.
 (74) Batcheller, S. A.; Tsumuraya, T.; Tempkin, O.; Davis, W. M.; Masamune, S. *J. Am. Chem. Soc.* **1990**, *112*, 9394.
 (75) Schafer, A.; Saak, W.; Weidenbruch, M.; Marsmann, H.; Henkel, G. *Chem. Ber./Recl.* **1997**, *130*, 1733.
 (76) Gritsenko, O. V.; Schipper, P. R. T.; Baerends, E. J. *Chem. Phys. Lett.* **1999**, *302*, 199.
 (77) Schipper, P. R. T.; Gritsenko, O. V.; van Gisbergen, S. J. A.; Baerends, E. J. *J. Chem. Phys.* **2004**, *112*, 1344.

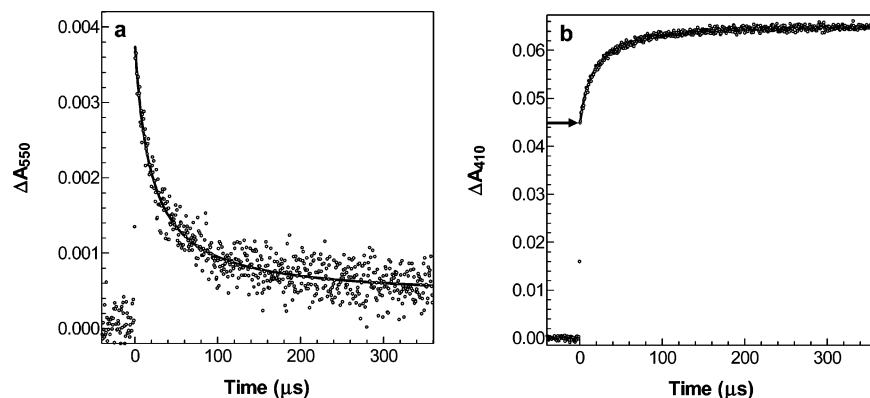


Figure 4. Transient decay/growth profiles recorded by laser flash photolysis of a 5×10^{-5} M solution of **15** in dried, deoxygenated hexane solution at 23 °C recorded at (a) 550 nm (Mes_2Ge) and (b) 410 nm (**6b**). The solid lines represent nonlinear least-squares fits to the second-order kinetic eqs 8 and 9, respectively. The arrow in part b indicates the initial ΔA value due to **6b** formed during the laser pulse.

Table 2. Calculated (TZ2P-PW91-SAOP-ZORA) and Experimental UV/vis Absorption Maxima for Dialkyl- and Diarylgermylenes and Their Digermene Dimers

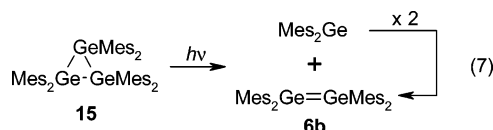
R	R_2Ge		$\text{R}_2\text{Ge}=\text{GeR}_2$	
	calcd [nm (eV)]	exptl [nm (eV)]	calcd [nm (eV)]	exptl [nm (eV)]
[C(SiMe ₃) ₂ CH ₂ -] (20)	462 (2.68)	450 (2.76) ^a		
H	493 (2.52)	514 (2.41) ^b	347 (3.57)	
Me	463 (2.68)	480 (2.58)	374 (3.32)	370 (3.35)
Ph	514 (2.41)	500 (2.48)	460 (2.70)	440 (2.82)
Mes	586 (2.19)	560 (2.23)	467 (2.66)	410 (3.03)

^a Reference 56. ^b Reference 79.

agreement in the position of the long-wavelength absorption maxima for most compounds. The largest deviation was obtained for **6b**; while the 0.37 eV difference is not unusual in TD-DFT spectroscopic calculations, the method failed to place the absorption maximum at shorter wavelengths than that of **6a**. The difficulties commonly encountered in the optimization of the structures of digermenes are presumably behind the limited accuracy of the calculated electronic structure and spectroscopic transitions in this case.

Absolute Rate Constants for Dimerization of Ph_2Ge and Mes_2Ge . As mentioned earlier, only qualitative agreement is observed between the decay kinetics of the three germylenes and the growth kinetics of the corresponding digermenes, with the decay of the germylene appearing to lag behind the formation of the digermene by a factor of ca. 2 in each case. Furthermore, the yield of **6b** via dimerization of Mes_2Ge appears to be significantly lower from **4b** than that observed previously using **15** as the precursor, although the quantum yield of Mes_2Ge appears to be higher.²⁵ We thus decided to reinvestigate the flash photolysis behavior of **15** in more detail, to ensure that a meaningful comparison of results from the two precursors would be possible. Photolysis of this compound affords Mes_2Ge and **6b** in equal initial amounts (eq 7), a feature which ultimately allows the dimerization kinetics of Mes_2Ge to be fully characterized, given a value of $\epsilon_{6b,410} = 20\,000$ for the extinction coefficient of **6b** at its long-wavelength absorption maximum.⁷⁸ It also allows the yield of **6b** via dimerization of Mes_2Ge to be determined with reasonable precision directly from the growth profile of the digermene.

The results obtained with this compound in the present work are in excellent agreement with those reported previously;²⁵ examples of typical decay/growth profiles for Mes_2Ge and **6b**



using **15** as the precursor are shown in Figure 4. The two sets of data exhibit excellent (nonlinear least squares) fits to second-order kinetics (equations 8 and 9), affording rate coefficients ($= 2k_{\text{dim}}[\text{Mes}_2\text{Ge}]_0$) of $(5.0 \pm 0.6) \times 10^4 \text{ s}^{-1}$ (Figure 4a) and $(6.1 \pm 0.2) \times 10^4 \text{ s}^{-1}$ (Figure 4b). The yield of **6b** formed via dimerization of Mes_2Ge from this precursor is given by twice the ratio of the best-fit values of $(\Delta A_{6b,\infty} - \Delta A_{6b,0})$ and $\Delta A_{6b,0}$; the results of 10 separate measurements afford an average value of $93 \pm 3\%$. Similar averaging of the initial ΔA_0 values for the germylene and digermene absorptions ($\Delta A_{\text{Mes}_2\text{Ge},0}$ and $\Delta A_{6b,0}$, respectively, recorded under conditions of constant laser intensity) leads to a value of $\epsilon_{6b,410}/\epsilon_{\text{Mes}_2\text{Ge},550} = 13.9 \pm 0.1$ for the ratio of the extinction coefficients due to **6b** and Mes_2Ge at their respective approximate absorption maxima. This yields a value of $\epsilon_{\text{Mes}_2\text{Ge},550} = 1440 \pm 400$ for the extinction coefficient of the germylene absorption at 550 nm, assuming an error of ca. 20% in the measured ϵ_{410} value for **6b**,⁷⁸ from which can be calculated an estimate of $k_{\text{dim}} = (5.4 \pm 1.5) \times 10^9 \text{ M}^{-1} \text{ s}^{-1}$ for the absolute rate constant for dimerization of Mes_2Ge in hexane solution at 23 °C. The average k_{dim} value obtained from the digermene data is ca. 15% larger than this, but the difference is well within the estimated error limits of the two determinations. The value of k_{dim} reported here for Mes_2Ge is quite similar to that reported by Conlin and co-workers for Mes_2Si under similar conditions ($k_{\text{dim}} = 8.5 \times 10^9 \text{ M}^{-1} \text{ s}^{-1}$ in cyclohexane at 25 °C).⁵⁴

$$\Delta A_{\text{Ar}_2\text{Ge},t} = \Delta A_{\text{Ar}_2\text{Ge},0}/(1 + 2k_{\text{dim}}[\text{Ar}_2\text{Ge}]_0t) \quad (8)$$

$$\Delta A_{6,t} = \Delta A_{6,0} + \Delta A_{6,\infty}\{1 - 1/(1 + 2k_{\text{dim}}[\text{Ar}_2\text{Ge}]_0t)\} \quad (9)$$

(78) Baines, K. M. Private communication.

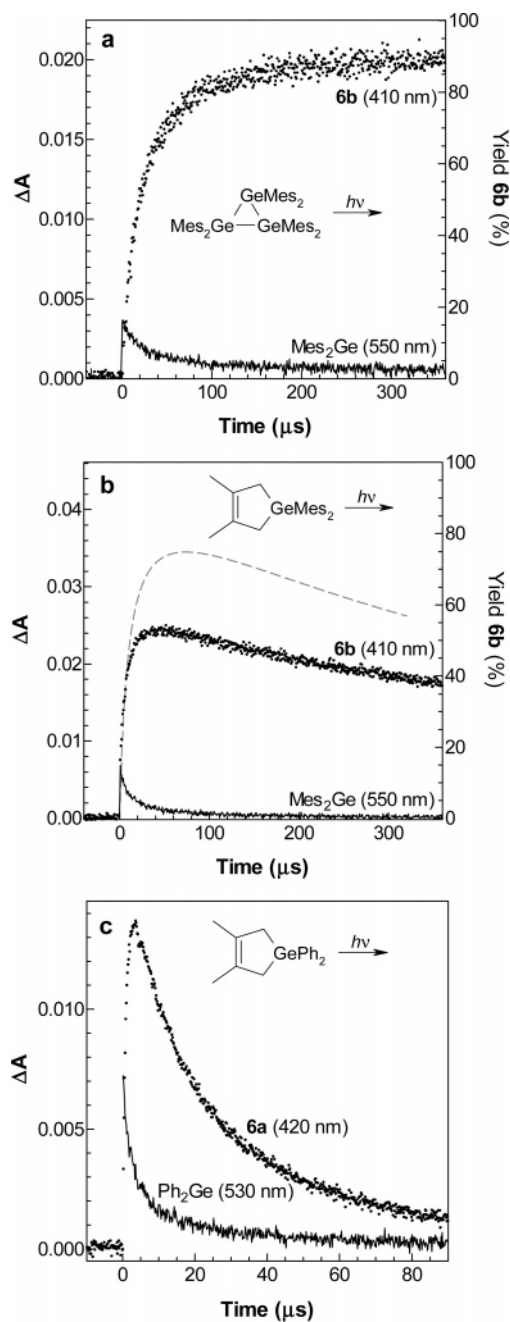


Figure 5. Transient decay/growth profiles recorded by laser flash photolysis of dried, deoxygenated hexane solutions of (a) **15** (7.0×10^{-5} M), (b) **4b** (0.0039 M), and (c) **4a** (0.0030 M) at the monitoring wavelengths indicated. All three solutions were optically matched at the excitation wavelength (248 nm). The 410 nm growth trace in part a is corrected for the initial ΔA value (ΔA_0) due to **6b** formed during the laser pulse (e.g., see Figure 4b). The plots of parts a and b were normalized against the ΔA_0 values of the germylene absorptions at 550 nm, to accentuate the differences in the dimerization yield of **6b** (right-hand axes) from the two precursors. The dashed gray line in part b is the simulated growth/decay curve for **6b**, assuming that Mes_2Ge undergoes exclusive dimerization and employing the extinction coefficients and rate constants given in the text for dimerization of Mes_2Ge and the subsequent decay of **6b**.

Figure 5 shows transient decay/growth profiles recorded by flash photolysis of optically matched (at 248 nm) solutions of **15** (7×10^{-5} M), **4b** (0.0039 M), and **4a** (0.0030 M) in dry, deoxygenated hexane under conditions of approximately constant laser intensity; the ΔA_{6b} data for **15** have been adjusted by subtracting the initial ΔA -value at 410 nm due to the portion

of **6b** formed during the laser pulse ($\Delta A_{6b,0}$ in eq 9), to facilitate comparison of the digermene growth profiles obtained from the two precursors. The data of Figure 5a and b have also been normalized against the initial $\Delta A_{\text{Mes}_2\text{Ge},0}$ values for the germylene transient absorptions at 550 nm for the two precursors, and then the plots have been scaled according to the predicted (100%) theoretical yield of digermene, to give an indication of the difference in the apparent yields of **6b** (as defined by the maximum ΔA_{6b} value in the growth profile) via germylene dimerization from **15** and **4b**. To help visualize the effect that the decay of **6b** has on its apparent yield in experiments with **4b** as precursor, kinetic simulations were carried out to model the time evolution of the digermene absorption, using the value of $[\text{Mes}_2\text{Ge}]_0$ defined by the germylene decay traces in Figure 5a and b and the extinction coefficients and k_{dim} value determined above, and working in the decay kinetics of the digermene signals determined over longer time scales from the two precursors. The simulated growth curve with no decay of the digermene included reproduced the data of Figure 5a quite closely, although (as it should) $\Delta A_{6b,\infty}$ levels off at a value corresponding to 100% yield, rather than the ca. 93% value exhibited by the actual data. The results of the simulation for **4b**, with the decay kinetics of the digermene included, are shown as the dashed curve in Figure 5b. They suggest that, with **4b** as precursor, there are one or more reactions of Mes_2Ge that compete with the formation of **6b** via dimerization, hence reducing the observed yield. The behavior exhibited using **15** as precursor allows us to rule out reaction with **6b** or solvent impurities, leaving reaction with something specific to the precursor, or its photochemistry as the most likely source of the competing process(es). Possible candidates are reaction of Mes_2Ge with **4b**, with a residual impurity from its synthesis, or with the photolysis coproduct, 2,3-dimethyl-1,3-butadiene (DMB). The reaction with **4b** can be ruled out on the basis of an experiment in which **4c** (as a model for the expected reactive site in **4b**, but transparent at the excitation wavelength) was added to solutions of **15**; the addition of up to 7.4 mM **4c** had no discernible effect on either the decay kinetics of Mes_2Ge or the yield or growth kinetics of **6b**, allowing an upper limit of $k < 5 \times 10^5 \text{ M}^{-1} \text{ s}^{-1}$ to be estimated for the rate constant for reaction of Mes_2Ge with precursor **4b**. Reaction of Mes_2Ge with the diene coproduct (DMB) also seems an unlikely possibility, but cannot be completely ruled out.³⁵ We are also unable to rule out the remaining possibility of impurity quenching; our sample of **4b** contains ca. 3% of an unknown impurity that we have been unable to remove. Given the nominal concentration of **4b** employed in our flash photolysis experiments (0.004 M), the impurity would be present at a concentration of ca. 10^{-4} M, roughly 10 times greater than the concentration of DMB produced in the laser pulse. Simulations indicate that, at this concentration, it would need to react with Mes_2Ge with a rate constant of ca. $3 \times 10^7 \text{ M}^{-1} \text{ s}^{-1}$ to reproduce the experimental growth/decay curve for **6b** with reasonable precision.

Figure 5c shows decay and growth traces for Ph_2Ge and **6a**, recorded over a 4-fold shorter time scale than the data for the mesityl system and at wavelengths to the red and blue of the absorption maxima due to the germylene and digermene, respectively, to minimize overlap in the decay/growth profiles. The decay trace shown for Ph_2Ge at 530 nm is expanded in Figure 6; it fits acceptably to second-order kinetics (equation

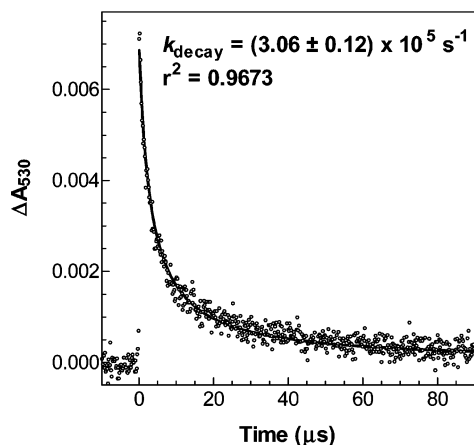


Figure 6. Transient decay trace recorded by laser flash photolysis of a 0.003 M solution of **4a** in dry, deoxygenated hexane at 23 °C. The solid line represents the best fit of the data to eq 8.

8), affording a rate coefficient ($=2k_{\text{dim}}[\text{Ph}_2\text{Ge}]_0$) of $(3.1 \pm 0.1) \times 10^5 \text{ s}^{-1}$. This leads to a value of $k_{\text{dim}} = (1.1 \pm 0.2) \times 10^{10} \text{ M}^{-1}\text{s}^{-1}$, using a value of $\epsilon_{\text{Ph}_2\text{Ge},530} = 990 \text{ M}^{-1}\text{cm}^{-1}$ (a factor of 0.60 of the $\epsilon_{\text{Ph}_2\text{Ge},500}$ value determined earlier) for the calculation of $[\text{Ph}_2\text{Ge}]_0$ from the initial ΔA -value at 530 nm. Comparison of the growth/decay data for **6a** to the results of kinetic simulations is not warranted in this case because of the lack of reliable extinction coefficient data for the digermene, as well as the fact that Ph_2Ge exhibits significantly higher reactivity than Mes_2Ge toward dienes,³⁵ and may also react with **6a** as it is formed. Nevertheless, it is clear from the data obtained for $\text{Mes}_2\text{Ge}/\mathbf{6b}$ that the maximum concentration of **6a** achieved from dimerization of Ph_2Ge (as measured by the maximum in the growth/decay curve) must be at least a factor of 2 lower than half the initial germylene concentration. This leads to the conclusion that the true extinction coefficient of **6a** at its absorption maximum must be at least 2 times greater than the value of ca. $6000 \text{ M}^{-1} \text{ cm}^{-1}$ estimated earlier by benzophenone actinometry.

Summary and Conclusions

1,1-Diphenylgermylene (Ph_2Ge) and its dimer, tetraphenyl-digermene (**6a**), have been detected and characterized in solution for the first time by laser flash photolysis methods. The germylene exhibits a weak long-wavelength UV/vis absorption at $\lambda_{\text{max}} = 500 \text{ nm}$ ($\epsilon_{\text{max}} = 1650 \pm 390 \text{ M}^{-1} \text{ cm}^{-1}$) and dimerizes with an absolute rate constant of ca. $1 \times 10^{10} \text{ M}^{-1} \text{ s}^{-1}$ in hexane solution at ambient temperatures to yield **6a**. The latter is a significantly stronger absorber, exhibiting $\lambda_{\text{max}} = 440 \text{ nm}$ ($\epsilon_{\text{max}} > 12\,000 \text{ M}^{-1} \text{ cm}^{-1}$) and decaying with mixed first- and second-order kinetics and $\tau \approx 40 \mu\text{s}$. Trapping experiments with methanol, acetic acid, isoprene, and triethylsilane afford the expected products of reaction of the germylene with the trapping reagent in essentially quantitative yield using conventional UV lamps as the excitation source. The product of 1,2-addition of MeOH to **6a** has been detected as well upon high-intensity laser photolysis of **4a**, under conditions where the germylene is produced in sufficiently high concentrations to allow dimerization of the species to compete with trapping by the alcohol.

Analogous results are obtained upon laser flash photolysis of the 1,1-dimesityl analogue **4b**, which yields the previously characterized Mes_2Ge . The latter dimerizes to yield the known

tetramesityldigermene (**6b**) with an absolute rate constant of ca. $6 \times 10^9 \text{ M}^{-1} \text{ s}^{-1}$. This is distinctly slower than the dimerization of Ph_2Ge , as might be expected, but the value indicates that steric effects on the rate constant for dimerization due to the mesityl substituents are relatively small. The somewhat lower reactivity of Mes_2Ge compared to Ph_2Ge is also reflected in the absolute rate constants for reaction of the two species with *n*-butylamine and acetic acid, both of which are potent germylene scavengers, reacting with absolute rate constants that are within a factor of 20 of the diffusion controlled rate in solution.

Analogous results to those for **4a** are also observed upon 193 nm laser flash photolysis of 1,1,3,4-tetramethylgermacyclopent-3-ene (**4c**) in hexane solution, affording a definitive UV/vis spectrum of Me_2Ge ($\lambda_{\text{max}} = 480 \text{ nm}$) in solution at ambient temperatures for the first time. The spectrum agrees well with that reported for Me_2Ge in the gas phase, but with only one of the several condensed phase spectra that have been assigned to this species previously. The transient dimerizes to yield the previously characterized tetramethyldigermene (**6c**, $\lambda_{\text{max}} = 370 \text{ nm}$), which then decays over several hundred microseconds. More complete characterization of Me_2Ge and **6c** must await the development of a more efficient photoprecursor that absorbs at longer wavelengths in the UV, so as to avoid the problems associated with far-UV excitation in solution. Work of this type is in progress in our laboratory.

The UV/vis spectra of all three germynes studied in this work, as well as those of digermenes **6a** and **6c** and the known stable germylene **20**, agree very closely with the results of time-dependent DFT calculations on the molecules, and also with the reported spectra of the corresponding silicon analogues. Close attention has been paid to the identification of the most appropriate basis sets used in the geometry optimizations and spectral calculations, not only to maximize the reliability of the results but also to ensure that the methods employed will be readily extendable to other di- and trivalent Group 14 reactive intermediates that are under investigation in our laboratory.

The present work demonstrates that the successful detection of reactive germynes in solution depends on several key factors. The most obvious of these is the photochemistry of the precursor(s) employed for generation of the species of interest, which for optimum results should be highly efficient and, more importantly, devoid of other competing photoreactions that produce (even minor amounts of) other reactive intermediates such as germanium-centered radicals or germenenes. Such species, particularly arylated derivatives, absorb much more strongly in the UV/visible spectrum than do germynes, whose long wavelength absorption bands are due to an orbitally forbidden (n,p) electronic transition and hence possess extinction coefficients on the order of only 10^3 . Another, perhaps less obvious factor is the experimental conditions employed for the experiment; in particular, the use of scrupulously dry solvents and glassware is *critical* for the successful observation of reactive germynes in solution. This is because scavenging of the species by water is rapid and *reversible*, which reduces the concentration of free germylene present in solution.³⁵ At the concentrations of water present in commercial, HPLC-grade hydrocarbon solvents, this results in much weaker transient signals than those observed under anhydrous conditions, for both the germylene and its digermene dimer, but has little effect on the apparent

lifetimes of the species. The use of flow techniques is also essential in methods requiring extensive signal averaging, as those employed here do. This results from the fact that the main fate of these species in the absence of scavengers is oligomerization, which yields products that absorb in the same range as the precursor and produce transient species of their own upon excitation. Finally, as our parallel study of the reactivity of Ph₂Ge shows in some detail,³⁵ simple diarylgermylenes are extremely potent electrophiles and react rapidly with even relatively weak nucleophiles, often to form Lewis acid–base complexes or other intermediates whose absorption spectra are blue-shifted relative to those of the free germylenes. We believe that factors of this type may well explain some of the discrepancies between the UV spectra reported here for Ph₂Ge and Me₂Ge and those reported previously, particularly those in low-temperature matrixes where diffusion of the free, photochemically generated germylene away from a weakly nucleophilic coproduct is inhibited.

Future work will explore the versatility of the germacyclopent-3-enyl system for the generation and study of other aryl- and alkylgermylene and digermene derivatives by laser flash photolysis methods.

Experimental Section

The procedures employed for the synthesis of **4a–c**, authentic samples of photoproducts, and semipreparative photolysis experiments, as well as detailed spectroscopic data for the compounds reported in this work, are described in the Supporting Information. Hexamethylcyclotrigermane was prepared according to the literature procedure⁸⁰ and recrystallized several times from hexanes.

Hexanes (EMD Omnisolv) was dried by refluxing for several days under argon over sodium/potassium amalgam followed by distillation. For 193 nm flash photolysis experiments, this procedure was preceded by repeated washing of the solvent with concentrated sulfuric acid, followed by distilled water and preliminary drying over anhydrous sodium sulfate. Deoxygenated samples of hexane used for 193 nm work exhibited an absorbance of no more than 0.3 at 193 nm in a 7 × 7 mm² quartz cell. *n*-Butylamine (Sigma-Aldrich) was refluxed for 12 h over potassium hydroxide and distilled. Glacial acetic acid was used as received from Sigma-Aldrich.

Laser flash photolysis experiments employed the pulses from a Lambda Physik Compex 120 excimer laser, filled with F₂/Kr/Ne (248 nm; ~25 ns; 100 ± 5 mJ) or F₂/Ar/Ne (193 nm; 20–25 ns; ca. 50 mJ) mixtures, and a Luzchem Research mLFP-111 laser flash photolysis system. The latter has been modified to incorporate an external 150 W high-pressure Xe lamp as monitoring source, powered by a Kratos LPS-251HR power supply, which provides a dynamic range in time of 10⁶ (1 μs to 1 s full scale). A Pyrex filter inserted between the sample cell and monochromator protects the PMT from scattered light from the laser when the monitoring wavelength is ≥330 nm; the excitation beam is delivered at a 90° angle relative to the monitoring beam through a 5 mm diameter circular slit, which defines the path length over which transients are produced. Solutions were prepared at concentrations such that the absorbance at the excitation wavelength (248 or 193 nm) was between ca. 0.7 and 0.9 and were flowed continuously through a thermostated 7 × 7 mm² Suprasil flow cell connected to a calibrated 100 mL reservoir, fitted with a glass frit to allow bubbling of nitrogen or argon gas through the solution for at least 30 min prior to and then throughout the duration of each experiment. The glassware, sample cells, and transfer lines used for these experiments were stored in a 65 °C vacuum oven when not in use, and the oven was vented with dry

nitrogen just prior to assembling the sample-handling system at the beginning of an experiment. Solution temperatures were measured with a Teflon-coated copper/constantan thermocouple inserted directly into the flow cell. Transient decay and growth rate constants were calculated by nonlinear least-squares analysis of the absorbance-time profiles using the Prism 3.0 software package (GraphPad Software, Inc.) and the appropriate user-defined fitting equations, after importing the raw data from the Luzchem mLFP software. Reagents were added directly to the reservoir by microliter syringe as aliquots of standard solutions. Rate constants were calculated by linear least-squares analysis of decay rate–concentration data (5–7 points) that spanned as large a range in transient decay rate as possible. Errors are quoted as twice the standard deviation obtained from the least-squares analyses.

The quantum yield for formation of methoxydiphenylgermane (**9a**) was determined by merry-go-round photolysis of deoxygenated, optically matched solutions of **4a** (0.037 M) and 1,1-diphenylsilacyclobutane (**13**; 0.043 M) in methanolic (0.5 M) cyclohexane-*d*₁₂ solution, using a Rayonet photochemical reactor fitted with four RPR-2537 low-pressure Hg lamps. The photolyses were monitored as a function of time between 0 and ca. 25% conversion of **4a** by 600 MHz NMR spectroscopy, using the peak due to residual C₆D₁₁H as internal integration standard. The quantum yield was calculated from the relative slopes of concentration vs time plots for the formation of **9a** from **4a** and **14** from **13** (see Supporting Information) and the reported quantum yield for the latter reaction ($\Phi_{14} = 0.21 \pm 0.02^{40}$). The value reported for the formation of **9a** from **4a** ($\Phi_{9a} = 0.62 \pm 0.08$) is the average of triplicate determinations.

Determination of the extinction coefficient for the Ph₂Ge absorption at 500 nm was carried out by benzophenone actinometry, using the so-called intensity variation method.^{47,48} The substrate and actinometer solutions were optically matched at the laser wavelength (248 nm) to ensure equal light absorption, and both were flowed through the same sample cell for sequential measurement of $\Delta A_{\lambda,0}$ ($\lambda = 500$ and 525 nm for Ph₂Ge and the benzophenone triplet, respectively) values as a function of laser intensity, which was controlled using neutral density filters constructed from wire screens. Both solutions were deoxygenated prior to the measurements with a stream of nitrogen and restored to their original volumes at the end of the deoxygenation procedure with fresh (deoxygenated) hexane. The resulting plots of $\Delta A_{\lambda,0}$ vs laser intensity, from whose slopes was calculated the extinction coefficient of the Ph₂Ge absorption using values of $\Phi = 1.0$ and $\epsilon_{525\text{nm}} = 6250 \pm 1250 \text{ M}^{-1} \text{ cm}^{-1}$ for the benzophenone triplet⁴⁹ and the quantum yield for Ph₂Ge formation determined above, are included in the Supporting Information. The value obtained, $\epsilon_{500\text{nm}} = 1650 \pm 390 \text{ M}^{-1} \text{ cm}^{-1}$, is the average of duplicate determinations.

Computational Details. A. Molecular Structures. Calculations were performed with the ADF 2003.01 density functional theory package (SCM),^{81–83} Unless otherwise indicated, the calculation of model geometries was gradient-corrected with the exchange and correlation functionals of Perdew and Wang (PW91);⁸⁴ all basis functions were of triple- ζ quality and were composed of uncontracted Slater-type orbitals (STOs), including all core electrons and two auxiliary basis set of STOs for polarization.

(79) Saito, K.; Obi, K. *Chem. Phys.* **1994**, *187*, 381.

(80) Ando, W.; Tsumuraya, T. *J. Chem. Soc., Chem. Commun.* **1987**, 1514.

(81) te Velde, G.; Bickelhaupt, F. M.; van Gisbergen, S. J. A.; Fonseca Guerra, C.; Baerends, E. J.; Snijders, J. G.; Ziegler, T. *J. Comput. Chem.* **2001**, *22*, 931.

(82) Fonseca Guerra, C.; Snijders, J. G.; te Velde, G.; Baerends, E. J. *Theor. Chem. Acc.* **1998**, *99*, 391.

(83) Baerends, E. J.; Autschbach, J.; Berces, A.; Bo, C.; Boerrigter, P. M.; Cavallo, L.; Chong, D. P.; Deng, L.; Dickson, R. M.; Ellis, D. E.; Fan, L.; Fischer, T. H.; Fonseca Guerra, C.; van Gisbergen, S. J. A.; Groeneveld, J. A.; Gritsenko, O. V.; Gruning, M.; Harris, F. E.; van den Hoek, P.; Jacobsen, H.; van Kessel, G.; Kootstra, F.; van Lenthe, E.; Osinga, V. P.; Patchkovskii, S.; Philipsen, P. H. T.; Post, D.; Pye, C. C.; Ravenek, W.; Ros, P.; Schipper, P. R. T.; Schreckenbach, G.; Snijders, J. G.; Sola, M.; Swart, M.; Swerhone, D.; te Velde, G.; Vernooijs, P.; Versluis, L.; Visser, O.; van Wezenbeek, E.; Wiesenekker, G.; Wolff, S. K.; Woo, T. K.; Ziegler, T. ADF2003.01. Amsterdam, SCM.

(84) Perdew, J. P. *Phys. Rev. B* **1992**, *46*, 6671.

B. Spectroscopic Calculations. The method is based on the time-dependent extension of density functional theory (TD-DFT) implemented^{85–89} in the ADF package. The adiabatic local density approximation (ALDA) was used for the exchange–correlation kernel^{90,91} and the differentiated static LDA expression was used with the Vosko–Wilk–Nusair parametrization.⁹² For the exchange–correlation potentials in the zeroth-order KS equations, the excitation energies and oscillator strengths were obtained using the Davidson iterative diagonalization method.

-
- (85) Gross, E. K. U.; Kohn, W. *Adv. Quantum Chem.* **1990**, *21*, 255.
(86) Gross, E. K. U.; Ullrich, C. A.; Gossmann, U. J. *Density functional theory of time-dependent systems*; Plenum: New York, 1995; p 149.
(87) Gross, E. K. U.; Dobson, J. F.; Petersilka, M. *Density Functional Theory*; Springer: Heidelberg, 1996.
(88) van Gisbergen, S. J. A.; Snijders, J. G.; Baerends, E. J. *J. Chem. Phys.* **1995**, *103*, 9347.
(89) van Gisbergen, S. J. A.; Snijders, J. G.; Baerends, E. J. *Comput. Phys. Commun.* **1999**, *118*, 119.
(90) van Gisbergen, S. J. A.; Snijders, J. G.; Baerends, E. J. *Phys. Rev. Lett.* **1997**, *78*, 3097.
(91) van Gisbergen, S. J. A.; Snijders, J. G.; Baerends, E. J. *J. Chem. Phys.* **1998**, *109*, 10644.
(92) Vosko, S. H.; Wilk, L.; Nusair, M. *Can. J. Phys.* **1980**, *58*, 1200.

Kinetic simulations were carried out using KinTekSim version 3.0.3 (KinTek Corp.).

Acknowledgment. We thank the Natural Sciences and Engineering Research Council of Canada, the Canada Foundation for Innovation, and the Ontario Innovation Trust for financial support; the McMaster Regional Centre for Mass Spectrometry for mass spectrometric analyses; and Professor M. Kira for providing the original spectroscopic data for germylene **20** and its silicon and tin congeners.

Supporting Information Available: Details of the synthesis and characterization of compounds and photoproducts, quantum yield and transient extinction coefficient data for Ph₂Ge, and computational details for the germylenes and digermenes studied in this work. This material is available free of charge via the Internet at <http://pubs.acs.org>.

JA046308Y